

Revisiting models that enhance $B^+ \rightarrow K^+ \nu \bar{\nu}$ in light of the new Belle II measurement

Xiao-Gang He,^{1,2,*} Xiao-Dong Ma,^{3,4,5,†} and German Valencia^{6,‡}

¹*Tsung-Dao Lee Institute (TDLI) & School of Physics and Astronomy (SPA),
Shanghai Jiao Tong University (SJTU), Shanghai 200240, China*

²*Department of Physics, National Taiwan University, Taipei 10617*

³*Key Laboratory of Atomic and Subatomic Structure and Quantum Control (MOE),
Institute of Quantum Matter, South China Normal University, Guangzhou 510006, China*

⁴*Guangdong Provincial Key Laboratory of Nuclear Science, Institute of Quantum Matter,
South China Normal University, Guangzhou 510006, China*

⁵*Guangdong-Hong Kong Joint Laboratory of Quantum Matter,
Southern Nuclear Science Computing Center,
South China Normal University, Guangzhou 510006, China*

⁶*School of Physics and Astronomy, Monash University,
Wellington Road, Clayton, VIC-3800, Australia*

Abstract

Belle II has recently reported the new measurement $\mathcal{B}(B^+ \rightarrow K^+ \nu \bar{\nu}) = (2.4 \pm 0.7) \times 10^{-5}$ [1] which is two times larger than their previous result (although consistent within errors) and about 2.8σ higher than the SM prediction. We re-examine new physics scenarios we have discussed previously which can enhance this rate to determine if they can accommodate the higher value reported in the new measurement. We use consistency with existing bounds on $B \rightarrow K^* \nu \bar{\nu}$, $b \rightarrow s \ell^+ \ell^-$ and B_s mixing to limit possible explanations for the excess. For the case of LFV neutrino couplings, we find that only two leptoquarks remain viable requiring a large $C_{9'}^{\tau\tau} = -C_{10'}^{\tau\tau}$. For models with different types of light dark matter particle pairs (scalar, fermion, or vector), the preliminary q^2 distribution from Belle II, which shows that the excess appears mostly for bins with $3 \leq q^2 \leq 7$ GeV² [2], implies only the vector current operators with scalar or vector dark matter particles with masses in the hundreds of MeV can match the anomaly.

*Electronic address: hexg@phys.ntu.edu.tw

†Electronic address: maxid@scnu.edu.cn

‡Electronic address: german.valencia@monash.edu

Contents

I. Introduction	3
II. Altering the properties of the neutrinos	4
III. Light-dark matter scenario for $B \rightarrow K + invisible$	8
A. Scalar DM case	9
B. Fermion DM case	10
C. Vector DM case	11
D. The q^2 distribution	12
IV. Summary and Conclusions	13
Acknowledgments	14
A. The differential width for $B \rightarrow K^{(*)}\chi\chi$	14
References	15

I. INTRODUCTION

The $B \rightarrow K^{(*)}\nu\bar{\nu}$ decays are amongst the cleanest modes to search for new physics due to their well-controlled theoretical uncertainty in the standard model (SM). A recent measurement by the Belle II collaboration finds a branching ratio [1]

$$\mathcal{B}(B^+ \rightarrow K^+\nu\bar{\nu})_{\text{exp}} = (2.4 \pm 0.7) \times 10^{-5}, \quad (1)$$

which is higher than SM expectation by about 2.8σ . This result is also about twice as large, but consistent within errors, with a previous Belle II combination $\mathcal{B}(B^+ \rightarrow K^+\nu\bar{\nu})_{\text{exp}}^{2021} = (1.1 \pm 0.4) \times 10^{-5}$ [3], and a new private average $\mathcal{B}(B^+ \rightarrow K^+\nu\bar{\nu})_{\text{exp}}^{\text{ave}} = (1.4 \pm 0.4) \times 10^{-5}$ presented in [1]. Currently, these numbers suggest consistency with the SM prediction [4],¹

$$\mathcal{B}(B^+ \rightarrow K^+\nu\bar{\nu})_{\text{SM}} = (4.43 \pm 0.31) \times 10^{-5}, \quad (2)$$

but the new measurement is sufficiently intriguing to entertain the possibility of new physics affecting this decay [5–10]. It has been noted that the CKM dependence of the SM prediction, which can hide new physics (NP), can be bypassed by considering certain ratios instead [11].

We have previously studied three different new physics scenarios that can enhance the rate for this mode: lepton flavour violating neutrino couplings (possibly induced by leptoquarks); a light sterile neutrino; or other invisible light particles (dark matter). These three cases exploit the fact that the neutrinos (or their flavour) are not detected so they could be mimicked by other unseen particles.

In this paper, we revisit those scenarios with the new (high) measurement in mind. Specifically, we want to explore whether this large value of $\mathcal{B}(B^+ \rightarrow K^+\nu\bar{\nu})$ (or indeed $B^+ \rightarrow K^+ + \cancel{E}$) can be accommodated in any of those scenarios while satisfying the existing upper bounds on $\mathcal{B}(B \rightarrow K^*\nu\bar{\nu})$ (again, more generally, $B \rightarrow K^* + \cancel{E}$). All these NP scenarios introduce correlations with other modes that also need to be considered.

Specifically, we will base our numerical study on the new measurement, Eq. (1) through the ratio

$$R_{\nu\nu}^K = \frac{\mathcal{B}(B^+ \rightarrow K^+\nu\bar{\nu})}{\mathcal{B}(B^+ \rightarrow K^+\nu\bar{\nu})_{\text{SM}}} = 5.4 \pm 1.6. \quad (3)$$

We will refer to this number as the “new 1σ range”. To discuss correlations with $R_{K^*}^{\nu\nu}$ we will use two numbers:

$$R_{K^*}^{\nu\nu} = \frac{\mathcal{B}(B \rightarrow K^*\nu\bar{\nu})}{\mathcal{B}(B \rightarrow K^*\nu\bar{\nu})_{\text{SM}}} \leq 2.7 \text{ or } 1.9. \quad (4)$$

The first number (2.7) arises from the combined charged and neutral modes and is directly quoted by the Belle collaboration [12]. The second number reflects the fact that the predictions for the

¹ Subtracting the so-called tree-level contribution.

decay rates of the charged and neutral modes are the same in all the models we consider. This suggests using instead the strongest experimental constraint, which in this case occurs for the neutral mode [12]

$$\mathcal{B}(B^0 \rightarrow K^{0*} \nu \bar{\nu}) \leq 1.8 \times 10^{-5} \text{ (90\% c.l.)}. \quad (5)$$

In combination with the corresponding SM prediction, this results in the second number (1.9) in Eq. (4).

The overall picture suggested by these numbers is that the new Belle II measurement does not imply significant changes to the averages yet. However, it invites us to entertain the possibility of a larger $R_K^{\nu\nu}$ and to study its implications for phenomenology, in particular for the implied $R_K^{\nu\nu} > R_{K^*}^{\nu\nu}$. That is the subject of this paper.

II. ALTERING THE PROPERTIES OF THE NEUTRINOS

We parameterise possible new physics entering these decays through an effective Hamiltonian at the b mass scale with dimension six operators responsible for $b \rightarrow s \nu \bar{\nu}$ in the low energy effective field theory approach (LEFT) [13, 14]. The effective theory originates in extensions of the SM containing new particles at or above the electroweak scale that have been integrated out but also allowing for the possibility of light right-handed neutrinos. Specifically, we consider the effective Hamiltonian

$$\mathcal{H}_{\text{NP}} = -\frac{4G_F}{\sqrt{2}} V_{tb} V_{ts}^* \frac{e^2}{16\pi^2} \sum_{ij} (C_L^{ij} \mathcal{O}_L^{ij} + C_R^{ij} \mathcal{O}_R^{ij} + C_L^{\prime ij} \mathcal{O}_L^{\prime ij} + C_R^{\prime ij} \mathcal{O}_R^{\prime ij}) + \text{h.c.}, \quad (6)$$

including the operators

$$\begin{aligned} \mathcal{O}_L^{ij} &= (\bar{s}_L \gamma_\mu b_L) (\bar{\nu}_i \gamma^\mu (1 - \gamma_5) \nu_j), & \mathcal{O}_R^{ij} &= (\bar{s}_R \gamma_\mu b_R) (\bar{\nu}_i \gamma^\mu (1 - \gamma_5) \nu_j), \\ \mathcal{O}_L^{\prime ij} &= (\bar{s}_L \gamma_\mu b_L) (\bar{\nu}_i \gamma^\mu (1 + \gamma_5) \nu_j), & \mathcal{O}_R^{\prime ij} &= (\bar{s}_R \gamma_\mu b_R) (\bar{\nu}_i \gamma^\mu (1 + \gamma_5) \nu_j). \end{aligned} \quad (7)$$

The Wilson coefficients in Eq. (7) are defined so that they only contain NP contributions. The SM contributes only to C_L^{ii} and is accounted for separately [15, 16]

$$C_{L \text{ SM}} = -\frac{X(x_t)}{s_W^2}, \quad X(x_t) = 1.469 \pm 0.017. \quad (8)$$

New interactions that conserve lepton number and have no new light particles can generate $\mathcal{O}_{L,R}^{ij}$. In contrast, the operators $\mathcal{O}_{L,R}^{\prime ij}$ are present when there are light right-handed neutrinos. Off diagonal (lepton flavour violating) operators occur for example, in models with leptoquarks. Other possibilities, such as scalar or tensor operators, are not discussed here.

Eq. (6) has contributions to $B \rightarrow K^{(*)} \nu \bar{\nu}$ that interfere with the SM, $\mathcal{O}_{L,R}^{ii}$; and others that do not, $\mathcal{O}_{L,R}^{i \neq j}$ and $\mathcal{O}_{L,R}^{\prime ij}$. In $B \rightarrow K \nu \bar{\nu}$ only the vector current enters the hadronic matrix element

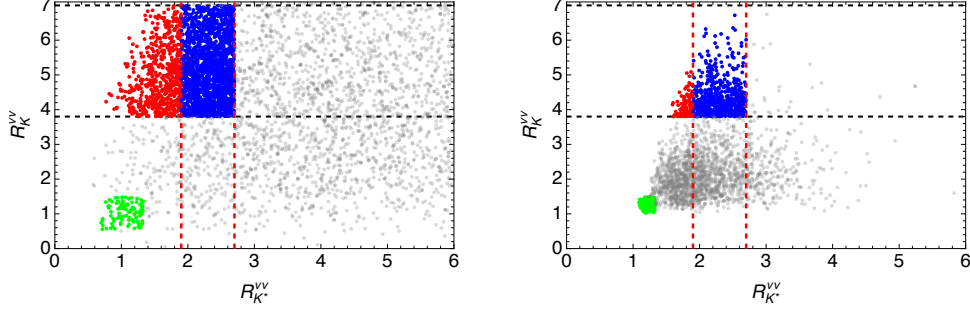


FIG. 1: The correlation between $R_K^{\nu\nu}$ and $R_{K^*}^{\nu\nu}$ scanning the 12 parameters C_L^{ij}, C_R^{ij} is shown in the left panel. The figure highlights in green those points that fall within 3σ of the SM. The points highlighted in blue or red fall within the new 1σ range of $R_K^{\nu\nu}$ (also marked by the horizontal dashed black lines). Additionally, the blue (red) points satisfy $R_{K^*}^{\nu\nu} \leq 2.7$ (1.9) respectively (values marked by the vertical dashed red lines). The right panel shows the equivalent scan for the 12 parameters $C_L'^{ij}, C_R'^{ij}$.

making the contributions to the rate from \mathcal{O}_L^{ij} and \mathcal{O}_R^{ij} (or from $\mathcal{O}_L'^{ij}$ and $\mathcal{O}_R'^{ij}$) the same. In $B \rightarrow K^* \nu \bar{\nu}$ both the vector and axial-vector currents enter the hadronic matrix element resulting in different contributions from \mathcal{O}_L^{ij} and \mathcal{O}_R^{ij} as well as from $\mathcal{O}_L'^{ij}$ and $\mathcal{O}_R'^{ij}$. The different neutrino chirality eliminates interference between the contributions from primed and un-primed operators for massless neutrinos. The corresponding ratios have been evaluated numerically in [17] using *flavio* [18], and found to be approximately

$$\begin{aligned}
 R_K^{\nu\nu} &\approx 1 - 0.1 \operatorname{Re} \sum_i (C_L^{ii} + C_R^{ii}) + 0.008 \sum_{ij} \left(|C_L^{ij} + C_R^{ij}|^2 + |C_L'^{ij} + C_R'^{ij}|^2 \right), \\
 R_{K^*}^{\nu\nu} &\approx 1 + \operatorname{Re} \sum_i (-0.1 C_L^{ii} + 0.07 C_R^{ii}) \\
 &\quad + \sum_{ij} \left[0.008 (C_L^{ij2} + C_R^{ij2} + C_L'^{ij2} + C_R'^{ij2}) - 0.01 (C_L^{ij} C_R^{ij} + C_L'^{ij} C_R'^{ij}) \right]. \quad (9)
 \end{aligned}$$

We begin by examining the correlations between $R_K^{\nu\nu}$ and $R_{K^*}^{\nu\nu}$ implied by Eq. (9) in light of the new 1σ range. These are illustrated in Fig. 1 for a scan of the 12 parameter space C_L^{ij}, C_R^{ij} in the left panel, and for the 12 parameter space $C_L'^{ij}, C_R'^{ij}$ in the right panel. The primed operators do not interfere with the SM as can be seen in the right panel, where all the points satisfy $R_{K^*}^{\nu\nu} \geq 1$ unlike the ones in the left panel. Since there is no interference between the primed and unprimed coefficients (we ignore neutrino masses) it will suffice to look at them separately. We focus on two groups that reproduce the new 1σ range of $R_K^{\nu\nu}$, $3.8 \leq R_K^{\nu\nu} \leq 7$. For one group, the blue points, $R_{K^*}^{\nu\nu} \leq 2.7$ and for the second group, the red points, $R_{K^*}^{\nu\nu} \leq 1.9$. For comparison, we also show in green, points that fall within 3σ of the corresponding SM predictions.² Whereas it is relatively easy to reproduce the new 1σ range of $R_K^{\nu\nu}$, it is harder to simultaneously obtain a low value of $R_{K^*}^{\nu\nu}$, closer to its SM value, this being more noticeable for the primed coefficients. Below, we

² Note that we have deliberately under-sampled the region not corresponding to the highlighted groups, which are shown as grey points.

explore this further within the models previously discussed in [17].

Models discussed in [17] that generate the operators with left-handed neutrinos, $\mathcal{O}_{L,R}^{ij}$, consist of scalar S and vector V leptoquarks coupling to SM fermions [19, 20],

$$\begin{aligned}\mathcal{L}_S &= \lambda_{LS_0} \bar{q}_L^c i\tau_2 \ell_L S_0^\dagger + \lambda_{L\tilde{S}_{1/2}} \bar{d}_R \ell_L \tilde{S}_{1/2}^\dagger + \lambda_{LS_1} \bar{q}_L^c i\tau_2 \vec{\tau} \cdot \vec{S}_1^\dagger \ell_L + \text{h. c.}, \\ \mathcal{L}_V &= \lambda_{LV_{1/2}} \bar{d}_R^c \gamma_\mu \ell_L V_{1/2}^{\dagger\mu} + \lambda_{LV_1} \bar{q}_L \gamma_\mu \vec{\tau} \cdot \vec{V}_1^{\dagger\mu} \ell_L + \text{h. c.}\end{aligned}\quad (10)$$

The leptoquark fields appearing in Eq. (10), and their transformation properties under the SM group, are

$$\begin{aligned}S_0^\dagger &= S_0^{1/3} : (\bar{3}, 1, 1/3), \quad \tilde{S}_{1/2}^\dagger = (\tilde{S}_{1/2}^{-1/3}, \tilde{S}_{1/2}^{2/3}) : (3, 2, 1/6), \\ \vec{\tau} \cdot \vec{S}_1^\dagger &= \begin{pmatrix} S_1^{1/3} & \sqrt{2} S_1^{4/3} \\ \sqrt{2} S_1^{-2/3} & -S_1^{1/3} \end{pmatrix} : (\bar{3}, 3, 1/3), \\ V_{1/2}^\dagger &= (V_{1/2}^{1/3}, V_{1/2}^{4/3}) : (\bar{3}, 2, 5/6), \quad \vec{\tau} \cdot \vec{V}_1^\dagger = \begin{pmatrix} V_1^{2/3} & \sqrt{2} V_1^{5/3} \\ \sqrt{2} V_1^{-1/3} & -V_1^{2/3} \end{pmatrix} : (3, 3, 2/3).\end{aligned}\quad (11)$$

Exchange of S_0, S_1 or V_1 , generates only C_L coefficients, whereas $\tilde{S}_{1/2}$ or $V_{1/2}$ generates only C_R coefficients. We find that it is not possible to satisfy the bound on $R_{K^*}^{\nu\nu}$, Eq. (4), in models with only C_L^{ij} coefficients because for the region where $3.8 \leq R_K^{\nu\nu} \leq 7$, there is a lower bound $R_{K^*}^{\nu\nu} \geq 3.8$. Models with only S_0, S_1 or V_1 are thus incompatible with the new measurement.

For the case with only C_R coefficients, on the other hand, there is a large region of parameter space that simultaneously satisfies the new 1σ range of $R_K^{\nu\nu}$ and the 90% c.l. upper bound on $R_{K^*}^{\nu\nu}$. However, if we restrict ourselves to models where only the off-diagonal (in lepton flavour) coefficients, $C_R^{i \neq j}$, are not zero, it is impossible to satisfy both constraints simultaneously because this scenario results in $R_K^{\nu\nu} = R_{K^*}^{\nu\nu}$.

We are left with two leptoquarks that can satisfy both the new 1σ range of $R_K^{\nu\nu}$ and the 90% c.l. upper bounds on $R_{K^*}^{\nu\nu}$. They are $\tilde{S}_{1/2}$ and $V_{1/2}$ with both diagonal and off diagonal flavour couplings. They generate the coefficients [17]

$$C_R^{ij} = C_{9'}^{ij} = -C_{10'}^{ij} = \frac{\pi}{\sqrt{2}\alpha G_F V_{tb} V_{ts}^*} \left(-\frac{\lambda_{L\tilde{S}_{1/2}}^{2j} \lambda_{L\tilde{S}_{1/2}}^{*3i}}{2m_{\tilde{S}_{1/2}}^2} + \frac{\lambda_{LV_{1/2}}^{3j} \lambda_{LV_{1/2}}^{*2i}}{m_{V_{1/2}}^2} \right), \quad (12)$$

and are thus correlated with other modes with charged leptons [21, 22]. The flavour diagonal entries for the first two generations affect the $b \rightarrow s\ell^+\ell^-$ processes that have long shown discrepancies with the SM. Typical global fits³ to $b \rightarrow s\ell^+\ell^-$ find preferred values $C_9^{\mu\mu} \sim C_9^{ee} \sim -1$ and allow $C_{9'}^{ii}$ and $C_{10'}^{ii}$ to be non-zero, but much smaller. This makes it obvious that $\tilde{S}_{1/2}$ and $V_{1/2}$ are not a preferred solution for the global fits to $b \rightarrow s\ell^+\ell^-$ observables. $\tilde{S}_{1/2}$ and $V_{1/2}$ can still

³ After the corrected LHCb value of $R_{K(K^*)}$ [23], for a review with references see [24].

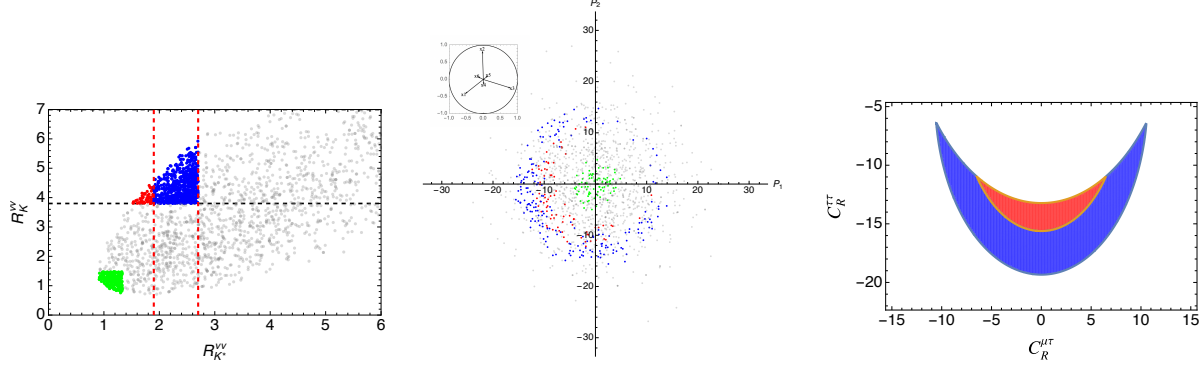


FIG. 2: Left panel: scan of parameters C_R^{ij} with the same color code as in Fig. 1. Centre panel: a selected slice of a projection in parameter space illustrating the location of the red and blue clusters. As this figure suggests, these clusters concentrate in regions where at least one of the diagonal entries $|C_R^{ii}|$ is near 10. Right panel: parameter region allowed when only $C_R^{\tau\tau}$ and $C_R^{\mu\tau}$ are non-zero.

modify $R_K^{\nu\nu}$ and $R_K^{\nu\nu*}$ but they are constrained by small values of $C_{9'}^{\mu\nu,ee}$ and $C_{10'}^{\mu\mu,ee}$ and additional NP would be needed to provide the preferred values of C_9 .

A scan of the six-parameter space for a symmetric C_R^{ij} is shown on the left panel of Fig. 2, marking as before the regions that satisfy Eq. (3) and Eq. (4). With the aid of tools described in [25–27] we can examine the parameter region responsible for the blue and red regions. We show in the centre panel a slice of a projection mostly onto the diagonal elements C_R^{ii} (axes labeled $x_{1,2,3}$). The slice is thin in the orthogonal space, mostly the off-diagonal elements $C_R^{i\neq j}$. The inset represents the projection matrix corresponding to this view. The visualisation indicates that the red and blue points concentrate in regions where at least one diagonal C_R^{ii} element is large, $\mathcal{O}(10)$. Given that the global fits $b \rightarrow s\ell^+\ell^-$ do not admit solutions with large $C_{9',10'}^{ee,\mu\mu}$ we conclude that the case with large $C_R^{\tau\tau}$ is the only viable solution. For further illustration, we show the viable two-parameter space $C_R^{\mu\tau} - C_R^{\tau\tau}$ region on the right panel of the same figure (the colour code is the same throughout).

Quantitatively, in this case, we find a lower bound of $R_K^{\nu\nu*} \geq 1.5$ for the red region. It corresponds to $C_R^{\mu\tau} \sim C_R^{\tau\mu} \sim 0$ and $C_R^{\tau\tau} \sim -13.2$. Similar solutions exist for small but non-zero $C_R^{ee}, C_R^{\mu\mu} \sim \mathcal{O}(0.1)$ in combination with a large $C_R^{\tau\tau} \sim \mathcal{O}(10)$.

The Wilson coefficients generated by either one $\tilde{S}_{1/2}$ or $V_{1/2}$, Eq. (12), imply large rates for other B decay modes that we illustrate in Fig. 3. We see that the CLFV branching fractions $\mathcal{B}(B^+ \rightarrow K^+\mu^-\tau^+)$ and $\mathcal{B}(B_s \rightarrow \mu^-\tau^+)$ can reach values of 10^{-5} , which are within factors of two below their current experimental upper limits: 2.8×10^{-5} (90%) and 4.2×10^{-5} (95%) [28] respectively. Similarly, the branching ratios for the lepton flavour conserving modes $\mathcal{B}(B^+ \rightarrow K^+\tau^+\tau^-)$ and $\mathcal{B}(B_s \rightarrow \tau^+\tau^-)$ can reach values of a few times 10^{-6} or 10^{-5} respectively, whereas their current experimental upper limits are $\mathcal{B}(B^+ \rightarrow K^+\tau^+\tau^-) \leq 2.25 \times 10^{-3}$ (90%) and $\mathcal{B}(B_s \rightarrow \tau^+\tau^-) \leq 6.8 \times 10^{-3}$ (95%) [28].

We now turn our attention to models with a light sterile neutrino (that couples to SM fields via

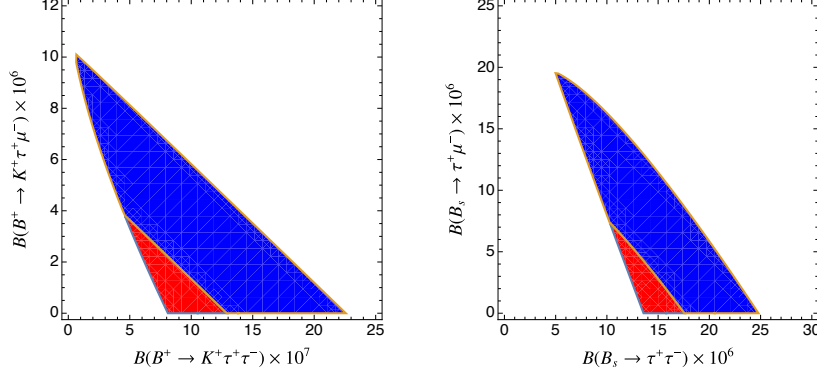


FIG. 3: Mapping of the parameter space selected in Fig. 2 into predictions for other B meson decay modes.

a Z') [29, 30]. This model produces non-zero $C_L'^{ij}, C_R'^{ij}$ as those in the right panel of Fig. 1. In this case, Eq. (9) implies that in the region where $3.8 \leq R_K^{\nu\nu} \leq 7$ there is a lower bound $R_{K^*}^{\nu\nu} \geq 1.47$, resulting in the reduced area covered by red points in the right panel of Fig. 1 relative to the left panel. Both $C_L'^{ij} \neq 0$ and $C_R'^{ij} \neq 0$ are needed to deviate from $R_K^{\nu\nu} = R_{K^*}^{\nu\nu}$ and the parameter scan shows that there could be solutions of this type. However, the specific model described in [17] is severely constrained by B_s mixing [31, 32]. When we take this constraint into consideration, the model cannot reproduce the 1σ range of the new measurement of $R_K^{\nu\nu}$ as illustrated in Fig. 4.

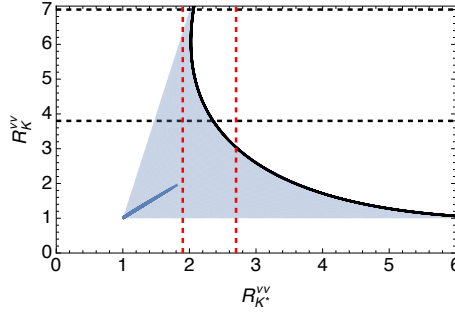


FIG. 4: Range of $R_K^{\nu\nu} - R_{K^*}^{\nu\nu}$ predictions covered by the two dimensional parameter space $|C_L'^{\tau\tau}| \leq 15$ and $|C_R'^{\tau\tau}| \leq 15$ shown in grey. The subspace that satisfies the B_s mixing constraints is the narrow darker blue region where $R_K^{\nu\nu} \approx R_{K^*}^{\nu\nu}$. This model cannot reach the new 1σ measurement of $R_K^{\nu\nu}$ and it is always below the upper bounds on $R_{K^*}^{\nu\nu}$.

III. LIGHT-DARK MATTER SCENARIO FOR $B \rightarrow K + \text{invisible}$

A large $\mathcal{B}(B^+ \rightarrow K^+ \nu \bar{\nu})$ as the one reported by Belle II can also be caused by invisible particles beyond the SM. In this case light-dark matter (DM) pairs take the place of the neutrinos, and we now examine this possibility.⁴ Since the spin of the possible DM particles is not known, we

⁴ Similar considerations for charm decay can be found in [33].

consider three cases: a spin-0 scalar ϕ , a spin-1/2 fermion χ , or a spin-1 vector X , respectively. We work within the framework of LEFT [14, 34], so we only impose the SM broken phase symmetry $SU(3)_c \times U(1)_{\text{em}}$ on the effective operators. In this way, the LEFT framework covers scenarios that contain both light DM as well as new weak scale mediators that have been integrated out. The complete LEFT operator basis with a pair of light DM fields at leading order was recently provided by us in Ref. [35]. In the following, we will adopt the notation in that paper and list the relevant FCNC local quark-DM operators mediating $B^+ \rightarrow K^+ + \text{invisible}$ decays for all cases.

For this discussion, it is not convenient to use the ratio $R_{\nu\nu}^K$ of Eq. (1). Instead, it is better to look at the difference between the measurement and the SM, and refer to it as the “NP window”,

$$\mathcal{B}(B^+ \rightarrow K^+ + \text{invisible})_{\text{NP}} \equiv \mathcal{B}(B^+ \rightarrow K^+ \nu \bar{\nu})_{\text{exp}} - \mathcal{B}(B^+ \rightarrow K^+ \nu \bar{\nu})_{\text{SM}} = (2.0 \pm 0.7) \times 10^{-5}. \quad (13)$$

In keeping with our previous discussion, we explore the possibility of attributing the new Belle II result to light dark particles while satisfying other constraints. We thus illustrate the implications of requiring the new contribution to the rate $B^+ \rightarrow K^+ + \text{invisible}$ to fall within the 1σ range of Eq. (13). At the same time, the effective operators studied below will also contribute to the decays $B^0 \rightarrow K^0 + \text{invisible}$ and $B^{+(0)} \rightarrow K^{*+(0)} + \text{invisible}$. There exist experimental upper bounds on these modes (at 90% c.l.) that we will use to constrain the parameter space. A final consideration relevant to this scenario is the observation by Belle II that the excess of events is predominantly concentrated in the region with $3 \leq q^2 \leq 7 \text{ GeV}^2$ [2].

A. Scalar DM case

We begin with the spin-0 scalar DM case. The leading order operators mediating $B^+ \rightarrow K^+ \phi \phi$ consist of quark scalar and vector currents with s, b flavors coupled to two scalar fields,

$$\mathcal{O}_{q\phi}^{S, sb} = (\bar{s}b)(\phi^\dagger \phi), \quad \mathcal{O}_{q\phi}^{V, sb} = (\bar{s}\gamma^\mu b)(\phi^\dagger i \overleftrightarrow{\partial}_\mu \phi), (\times) \quad (14)$$

The symbol “(\times)” indicates an operator that vanishes for real scalar fields, and $\phi^\dagger \overleftrightarrow{\partial}_\mu \phi \equiv \phi^\dagger (\partial_\mu \phi) - (\partial_\mu \phi^\dagger) \phi$. These operators occur at dimension six in the SMEFT framework [36]. In addition to $B^+ \rightarrow K^+ \phi \phi$, the scalar current operator also induces the decay $B^0 \rightarrow K^0 \phi \phi$. The vector operator can also mediate the modes $B^0 \rightarrow K^{*0} \phi \phi$ and $B^+ \rightarrow K^{*+} \phi \phi$. The differential decay widths for these four modes have been given in [35]. For the hadronic form factors involved, we use the recent lattice calculation in [37] for $B \rightarrow K$, and those from light-cone sum rule methods [38, 39] for $B \rightarrow K^*$. To quantify the allowed parameter space, we define an effective heavy scale associated with each operator as $C_{q\phi}^{S, sb} \equiv \Lambda_{\text{eff}}^{-1}$ and $C_{q\phi}^{V, sb} \equiv \Lambda_{\text{eff}}^{-2}$.

Fig. 5 shows our results for the operators in Eq. (14). The green (solid and dashed) lines and the blue dashed line mark the lower limit on the scale Λ_{eff} associated with the scalar (vector) operator in the left (right) panel resulting from the upper bound on $B^{+(0)} \rightarrow K^{*+(0)} \phi \phi$ and $B^0 \rightarrow K^0 \phi \phi$ respectively. The pink region covers the parameter space in the $m_\phi - \Lambda_{\text{eff}}$ plane that accommodates the Belle II 1σ range. The grey area is excluded by the experimental upper limits and is mostly

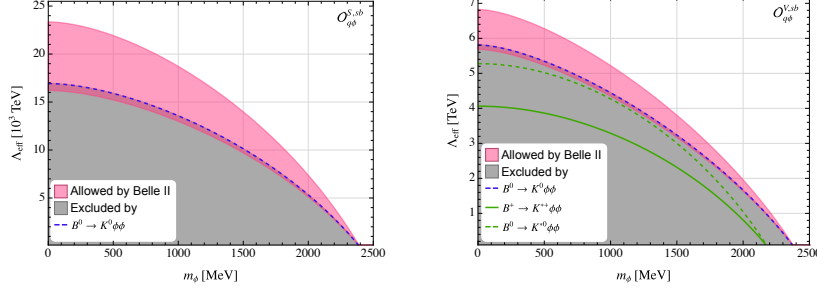


FIG. 5: The pink region is the parameter space that could explain the recent Belle II excess with scalar DM for scalar (vector) quark current operators $\mathcal{O}_{q\phi}^{S, sb}$ ($\mathcal{O}_{q\phi}^{V, sb}$). The grey region is excluded by other B meson decay modes that are indicated in the plots by colour lines.

due to the neutral modes $B^0 \rightarrow K^{(*)0} \nu \bar{\nu}$ for these two operators. The scalar operator provides a larger parameter region consistent with the new Belle II measurement than the vector operator. The vector operator, however, results in a q^2 distribution more in tune with the reported excess, as we illustrate in Fig. 8.

B. Fermion DM case

We now turn to fermion DM particles.⁵ Denoting the DM field by χ , there are six leading, dimension six operators that are responsible for the $B^+ \rightarrow K^+ \chi \chi$ transition [35],

$$\mathcal{O}_{q\chi 1}^{S, sb} = (\bar{s}b)(\bar{\chi}\chi), \quad \mathcal{O}_{q\chi 2}^{S, sb} = (\bar{s}b)(\bar{\chi}i\gamma_5\chi), \quad (15a)$$

$$\mathcal{O}_{q\chi 1}^{V, sb} = (\bar{s}\gamma^\mu b)(\bar{\chi}\gamma_\mu\chi), (\times) \quad \mathcal{O}_{q\chi 2}^{V, sb} = (\bar{s}\gamma^\mu b)(\bar{\chi}\gamma_\mu\gamma_5\chi), \quad (15b)$$

$$\mathcal{O}_{q\chi 1}^{T, sb} = (\bar{s}\sigma^{\mu\nu}b)(\bar{\chi}\sigma_{\mu\nu}\chi), (\times) \quad \mathcal{O}_{q\chi 2}^{T, sb} = (\bar{s}\sigma^{\mu\nu}b)(\bar{\chi}\sigma_{\mu\nu}\gamma_5\chi), (\times) \quad (15c)$$

where the “(\times)” indicates the accompanying operator vanishes for Majorana fermions. The implications for $B \rightarrow K$ transitions from such operators have been partially considered before [42]. In Ref. [42], only the charged processes $B^+ \rightarrow K^{(*)+} \chi \chi$ are considered and this was done before the new Belle II measurement. Here we use the new experimental result and include all possible modes including the neutral ones. We also use the new lattice form factors [37].

The differential decay widths for this case have not been presented previously in the literature, and we collect them in Appendix A for reference. To study the parameter space, we rewrite the Wilson coefficient C_i^j of the operator \mathcal{O}_i^j as an effective scale $C_i^j \equiv \Lambda_{\text{eff}}^{-2}$. For each operator in Eq. (15), Fig. 6 shows the parameter space in the $m_\chi - \Lambda_{\text{eff}}$ plane that reproduces the new Belle II 1σ result, the pink shaded region. The grey region is excluded by other B meson decay modes. It can be seen that the two operators with tensor quark currents have almost no viable region to explain the excess, unlike the operators with scalar or vector currents. Most of the exclusion for

⁵ A general study of the three-body decay with sterile neutrinos in the ν SMEFT framework [40] can be found in [8, 41].

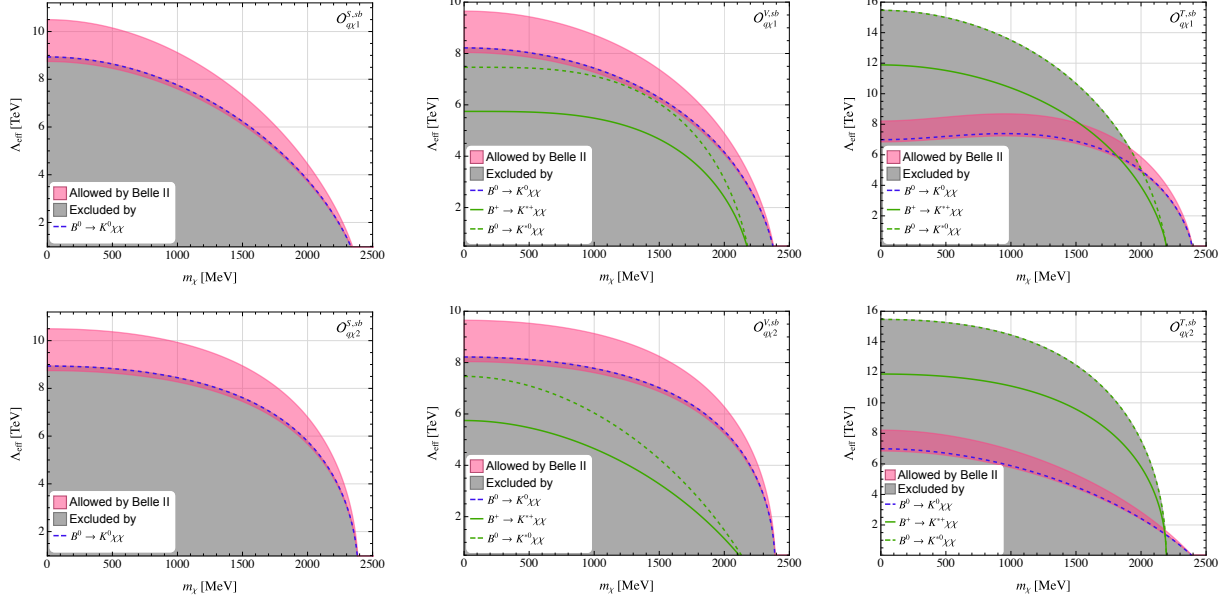


FIG. 6: The pink region shows the parameter space that could explain the recent Belle II excess with fermion DM for the operators in Eq. (15). The gray region is excluded by other B meson decay modes that are indicated in the plots by coloured lines.

these four operators arises from the upper limit on the neutral mode $B^0 \rightarrow K^0 \chi \chi$. If we insist on an excess of events concentrated in the $3 \leq q^2 \leq 7 \text{ GeV}^2$ bins, only the vector current operators $\mathcal{O}_{qX1,2}^{V,ab}$ with certain DM masses remain viable as we illustrate in Fig. 8.

C. Vector DM case

Finally, we consider the vector DM. There are two parametrizations that can be used in this case as discussed in [35]. Here we adopt the one with a four-vector field X_μ for simplicity. The operators have been classified by us in [35], and the ones relevant for $B^+ \rightarrow K^+ X X$ transitions are,

$$\mathcal{O}_{qX}^{S,ab} = (\bar{s}b)(X_\mu^\dagger X^\mu), \quad (16a)$$

$$\mathcal{O}_{qX1}^{T,ab} = \frac{i}{2}(\bar{s}\sigma^{\mu\nu}b)(X_\mu^\dagger X_\nu - X_\nu^\dagger X_\mu), (\times) \quad (16b)$$

$$\mathcal{O}_{qX2}^{T,ab} = \frac{1}{2}(\bar{s}\sigma^{\mu\nu}\gamma_5 b)(X_\mu^\dagger X_\nu - X_\nu^\dagger X_\mu), (\times) \quad (16c)$$

$$\mathcal{O}_{qX2}^{V,ab} = (\bar{s}\gamma_\mu b)\partial_\nu(X^{\mu\dagger}X^\nu + X^{\nu\dagger}X^\mu), \quad (16d)$$

$$\mathcal{O}_{qX3}^{V,ab} = (\bar{s}\gamma_\mu b)(X_\rho^\dagger \overleftrightarrow{\partial}_\nu X_\sigma)\epsilon^{\mu\nu\rho\sigma}, \quad (16e)$$

$$\mathcal{O}_{qX4}^{V,ab} = (\bar{s}\gamma^\mu b)(X_\nu^\dagger i\overleftrightarrow{\partial}_\mu X^\nu), (\times) \quad (16f)$$

$$\mathcal{O}_{qX5}^{V,ab} = (\bar{s}\gamma_\mu b)i\partial_\nu(X^{\mu\dagger}X^\nu - X^{\nu\dagger}X^\mu), (\times) \quad (16g)$$

$$\mathcal{O}_{qX6}^{V,ab} = (\bar{s}\gamma_\mu b)i\partial_\nu(X_\rho^\dagger X_\sigma)\epsilon^{\mu\nu\rho\sigma}. (\times) \quad (16h)$$

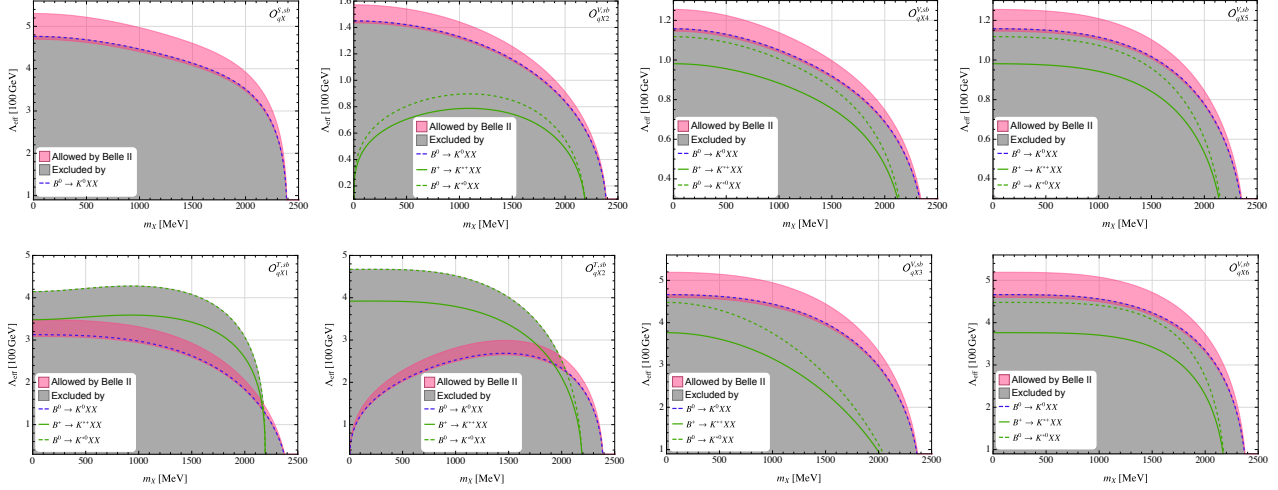


FIG. 7: The pink region shows the parameter space that could explain the recent Belle II excess with vector DM for the operators in Eq. (16). The grey region is excluded by other B meson decay modes that are indicated in the plots by coloured lines.

The symbol “(\times)” indicates that the corresponding operator vanishes for real vector fields. To address the well-known singularity problem that affects vector fields in the limit of vanishing mass, for our numerical analysis, we scale the Wilson coefficients of these operators in the following manner,

$$C_{qX}^S \equiv \frac{m^2}{\Lambda_{\text{eff}}^3}, \quad C_{qX1,2}^T \equiv \frac{m^2}{\Lambda_{\text{eff}}^3}, \quad C_{qX2,4,5}^V \equiv \frac{m^2}{\Lambda_{\text{eff}}^4}, \quad C_{qX3,6}^V \equiv \frac{m}{\Lambda_{\text{eff}}^3}. \quad (17)$$

In Fig. 7, we show the parameter space resulting in a branching ratio in agreement with Eq. (13). It can be seen, that except for the two operators with tensor quark currents $\mathcal{O}_{qX1,2}^{T,ab}$, the remaining operators contain a large acceptable parameter region.

D. The q^2 distribution

The excess of events observed by Belle II appears to occur mainly for q^2 values between 3 – 7 GeV^2 [1].⁶ It is thus interesting to compare the q^2 distributions that follow from the different DM cases. Because the new particles would add incoherently to the SM rate, we combine the two to obtain a normalized q^2 distribution as,

$$\frac{d\tilde{\Gamma}}{dq^2} \equiv \frac{\frac{d\Gamma_{\text{SM}}}{dq^2} + \frac{d\Gamma_{\text{NP}}}{dq^2}}{\Gamma_{\text{SM}} + \Gamma_{\text{NP}}} = \frac{\frac{d\tilde{\Gamma}_{\text{SM}}}{dq^2} + (R_{\nu\nu}^K - 1) \frac{d\tilde{\Gamma}_{\text{NP}}}{dq^2}}{R_{\nu\nu}^K}, \quad (18)$$

where $d\tilde{\Gamma}_{\text{SM,NP}}/dq^2 \equiv (d\Gamma_{\text{SM,NP}}/dq^2)/\Gamma_{\text{SM,NP}}$.

⁶ We thank Eldar Ganiev for confirming this observation.

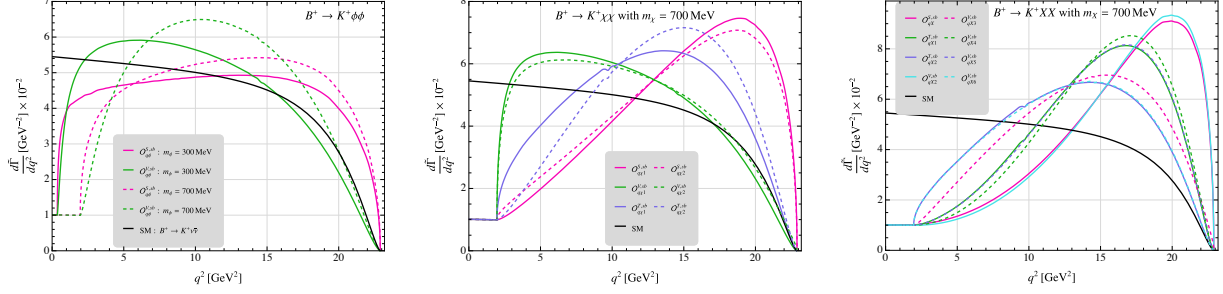


FIG. 8: The q^2 distribution of normalized differential decay widths from all three cases: scalar DM (left panel), fermion DM (middle panel), vector DM (right panel) for selected masses.

In Fig. 8, we show representative cases from the insertion of all the DM operators discussed above for selected DM mass value $m_\phi = 300, 700$ MeV (left panel), $m_\chi = 700$ MeV (centre panel) and $m_V = 700$ MeV (right panel). For comparison, the SM distribution is also shown (black line). The figures indicate that the cases of $\mathcal{O}_{q\phi}^{V, sb}$ with $m_\phi \sim 300$ MeV and $\mathcal{O}_{q\chi}^{V, sb}$ with $m_\chi \sim 700$ MeV would more closely match the preliminary q^2 distribution of the excess. The study of the shape of this distribution will help narrow down possible explanations if the excess is confirmed.

IV. SUMMARY AND CONCLUSIONS

The recent measurement of the branching ratio $\mathcal{B}(B^+ \rightarrow K^+ \nu \bar{\nu})$ by the Belle II collaboration is larger than the SM prediction at the 2.8σ level and has attracted some attention. Although this measurement is consistent within errors with previous ones and the resulting average is consistent with the SM within errors, it invites speculation on the possibility of accommodating a rate that exceeds the SM. In particular we studied whether models that can enhance $R_K^{\nu\nu}$ can remain consistent with a lower $R_{K^*}^{\nu\nu}$.

Since the neutrinos in the final state are not identified, it is possible to enhance $R_K^{\nu\nu}$ with models that contain other invisible particles, such as light dark matter. It is also possible to do so with additional neutrinos or by introducing lepton flavour violating neutrino couplings as in models previously discussed in the literature.

We began with a model-independent description of the interactions in $b \rightarrow s \nu \bar{\nu}$. We considered four dimension six operators, two of which interfere with the SM and two that do not. We then scanned the parameter spaces to see if it was possible to cover the new Belle II 1σ range for $\mathcal{B}(B^+ \rightarrow K^+ \nu \bar{\nu})$ as well as existing bounds on $\mathcal{B}(B \rightarrow K^* \nu \bar{\nu})$. Our results, shown in Figs 1 and 2 indicate that whereas it is relatively easy to reproduce the new 1σ range of $R_K^{\nu\nu}$, it is much harder to simultaneously obtain a low value of $R_{K^*}^{\nu\nu} < 1.9$. This conclusion is stronger for operators which have no interference with the SM. The relative size of $R_K^{\nu\nu}$ and $R_{K^*}^{\nu\nu}$ will play an important role in untangling any hint for NP in these modes.

We then restricted the parameter scans to models we had previously studied, and found that there is one scenario with $\tilde{S}_{1/2}$ or $V_{1/2}$ leptoquarks that can survive constraints from both $R_{K^*}^{\nu\nu}$

and $b \rightarrow s\ell^+\ell^-$ modes. It predicts significant enhancements for the modes $B^+ \rightarrow K^+\mu^-\tau^+$, $B_s \rightarrow \mu^-\tau^+$, $B^+ \rightarrow K^+\tau^-\tau^+$ and $B_s \rightarrow \tau^-\tau^+$. In contrast, we found that models with only C_L^{ij} coefficients, such as those with S_0, S_1 or V_1 leptoquarks, cannot satisfy both conditions on $R_K^{\nu\nu}$ and $R_{K^*}^{\nu\nu}$. We also found that solutions with light right-handed neutrinos that couple to SM fields via a Z' are excluded when B_s mixing constraints are imposed.

In scenarios with light dark matter resulting in $B^+ \rightarrow K^+ + \cancel{E}$, we present constraints on the effective scale of all lowest dimensional operators coupling b, s quark bilinears to pairs of scalar, fermion or vector dark matter particles. We find that existing experimental upper bounds on $B^0 \rightarrow K^0 + \cancel{E}$, $B^0 \rightarrow K^{0*} + \cancel{E}$ and $B^+ \rightarrow K^{+*} + \cancel{E}$ rule out much of the parameter space where these operators could enhance $B^+ \rightarrow K^+ + \cancel{E}$ to the level of the new Belle II result.

We illustrated the remaining parameter space that can survive the constraints, finding that the effective scales are typically constrained to be in the multi-TeV range for scalar and fermion dark matter. For vector dark matter, the effective scales are in the several hundred GeV range when the masses are less than 100 MeV and become weaker as the mass increases due to the reduced phase space.

We confronted the different operators with the preliminary q^2 distribution reported by Belle II. We found that three operators with specific values for dark matter mass would best accommodate the spectrum, $\mathcal{O}_{q\phi}^{V, sb}$ with $m_\phi \sim 300$ MeV and $\mathcal{O}_{q\chi 1,2}^{V, sb}$ with $m_\chi \sim 700$ MeV. Clearly, the experimental result is preliminary, but our exercise illustrates how the shape of the spectrum can be used to narrow the possible explanations for an excess in the rate.

Acknowledgments

GV and XGH were supported in part by the Australian Government through the Australian Research Council Discovery Project DP200101470. XGH was supported by the Fundamental Research Funds for the Central Universities, by the National Natural Science Foundation of the People's Republic of China (No. 12090064, No. 11735010, and No. 11985149), and by MOST 109- 2112-M-002-017-MY3. XDM was supported in part by the Guangdong Major Project of Basic and Applied Basic Research No. 2020B0301030008 and by the Grant No. NSFC-12305110.

Appendix A: The differential width for $B \rightarrow K^{(*)}\chi\chi$

For the light invisible fermionic DM case, based on the parametrization for the hadronic matrix elements given in [35, 38, 39, 43], the differential decay widths for $B \rightarrow K^+(K^0)\chi\chi$ and $B \rightarrow K^{*+}(K^{*0})\chi\chi$ transitions induced from the interactions in Eq. (15) are calculated to take the following general form,

$$\frac{d\Gamma_{B \rightarrow P\chi\chi}}{dq^2} = \frac{\lambda^{\frac{1}{2}}(m_B^2, m_P^2, s)\kappa^{\frac{1}{2}}(m^2, s)}{384\pi^3 m_B^3} \left\{ \frac{3(m_B^2 - m_P^2)^2}{(m_b - m_s)^2} f_0^2 \left[(s - 4m^2) \left| C_{q\chi 1}^{S, sb} \right|^2 + s \left| C_{q\chi 2}^{S, sb} \right|^2 \right] \right\}$$

$$\begin{aligned}
& + \frac{2(s+2m^2)\lambda(m_B^2, m_P^2, s)}{s} f_+^2 \left| C_{q\chi^1}^{V, sb} \right|^2 \\
& + \frac{2}{s} [6m^2(m_B^2 - m_P^2)^2 f_0^2 + (s-4m^2)\lambda(m_B^2, m_P^2, s) f_+^2] \left| C_{q\chi^2}^{V, sb} \right|^2 \\
& + \frac{4\lambda(m_B^2, m_P^2, s)}{(m_B + m_P)^2} f_T^2 \left[(s+8m^2) \left| C_{q\chi^1}^{T, sb} \right|^2 + (s-4m^2) \left| C_{q\chi^2}^{T, sb} \right|^2 \right] \\
& - \frac{12m(m_B^2 - m_P^2)^2}{m_b - m_s} f_0^2 \Im \left[C_{q\chi^2}^{S, sb} C_{q\chi^2}^{V, sb*} \right] + \frac{24m\lambda(m_B^2, m_P^2, s)}{m_B + m_P} f_+ f_T \Re \left[C_{q\chi^1}^{V, sb} C_{q\chi^1}^{T, sb*} \right] \Big\} \quad (A1) \\
\frac{d\Gamma_{B \rightarrow V \chi \chi}}{dq^2} & = \frac{\lambda^{\frac{3}{2}}(m_B^2, m_P^2, s) \kappa^{\frac{1}{2}}(m^2, s)}{96\pi^3 m_B^3 (m_B + m_V)^2} V_0^2 \left[(s+2m^2) \left| C_{q\chi^1}^{V, sb} \right|^2 + (s-4m^2) \left| C_{q\chi^2}^{V, sb} \right|^2 \right] \\
& + \frac{\lambda^{\frac{1}{2}}(m_B^2, m_V^2, s) \kappa^{\frac{1}{2}}(m^2, s)}{48\pi^3 m_B^3 s} \left\{ (s+8m^2)\lambda(m_B^2, m_V^2, s) T_1^2 \right. \\
& + (s-4m^4) \left[(m_B^2 - m_V^2)^2 T_2^2 + \frac{8m_B^2 m_V^2 s}{(m_B + m_V)^2} T_{23}^2 \right] \Big\} \left| C_{q\chi^1}^{T, sb} \right|^2 \\
& + \frac{\lambda^{\frac{1}{2}}(m_B^2, m_V^2, s) \kappa^{\frac{1}{2}}(m^2, s)}{48\pi^3 m_B^3 s} \left\{ (s-4m^2)\lambda(m_B^2, m_V^2, s) T_1^2 \right. \\
& + (s+8m^2) \left[(m_B^2 - m_V^2)^2 T_2^2 + \frac{8m_B^2 m_V^2 s}{(m_B + m_V)^2} T_{23}^2 \right] \Big\} \left| C_{q\chi^2}^{T, sb} \right|^2 \\
& + \frac{m\lambda^{\frac{3}{2}}(m_B^2, m_V^2, s) \kappa^{\frac{1}{2}}(m^2, s)}{8\pi^3 m_B^3 (m_B + m_V)} V_0 T_1 \Re \left[C_{q\chi^1}^{V, sb} C_{q\chi^1}^{T, sb*} \right]. \quad (A2)
\end{aligned}$$

where $P = K^+, K^0$ and $V = K^{*+}, K^{*0}$. C_i^j is the corresponding Wilson coefficient of the operator \mathcal{O}_i^j . The Källén function $\lambda(x, y, z) \equiv x^2 + y^2 + z^2 - 2(xy + yz + zx)$ and $\kappa(m^2, s) = \sqrt{1 - 4m^2/s}$, with m being the DM mass while s the invariant mass of DM pair. m_B, m_P, m_V are the masses of mesons B^+, P, V and m_b, m_s are masses of b, s quarks, respectively. $f_0, f_+, V_0, f_T, T_1, T_2, T_{23}$ are hadronic form factors associated with different quark currents, with definitions that can be found in [35, 43].

-
- [1] A. Glazov (2023), plenary talk given at the EPS-HEP2023 Conference in Hamburg (Germany), URL <https://indico.desy.de/event/34916/contributions/149769/attachments/84417/111854/Belle%20II%20highlights.pdf>.
 - [2] E. Ganiev (2023), parallel talk given at the EPS-HEP2023 Conference in Hamburg (Germany), URL https://indico.desy.de/event/34916/contributions/146877/attachments/84380/111798/EWP@Belle2_EPS.pdf.
 - [3] F. Dattola (Belle-II), in 55th Rencontres de Moriond on Electroweak Interactions and Unified Theories (2021), 2105.05754.
 - [4] D. Bečirević, G. Piazza, and O. Sumensari, Eur. Phys. J. C **83**, 252 (2023), 2301.06990.
 - [5] R. Bause, H. Gisbert, and G. Hiller (2023), 2309.00075.
 - [6] L. Allwicher, D. Becirevic, G. Piazza, S. Rosauero-Alcaraz, and O. Sumensari (2023), 2309.02246.
 - [7] P. Athron, R. Martinez, and C. Sierra (2023), 2308.13426.
 - [8] T. Felkl, A. Giri, R. Mohanta, and M. A. Schmidt (2023), 2309.02940.

- [9] M. Abdughani and Y. Reyimuaji (2023), 2309.03706.
- [10] H. K. Dreiner, J. Y. Günther, and Z. S. Wang (2023), 2309.03727.
- [11] A. J. Buras, Eur. Phys. J. C **83**, 66 (2023), 2209.03968.
- [12] J. Grygier et al. (Belle), Phys. Rev. D **96**, 091101 (2017), [Addendum: Phys.Rev.D 97, 099902 (2018)], 1702.03224.
- [13] B. Grzadkowski, M. Iskrzynski, M. Misiak, and J. Rosiek, JHEP **10**, 085 (2010), 1008.4884.
- [14] E. E. Jenkins, A. V. Manohar, and P. Stoffer, JHEP **03**, 016 (2018), 1709.04486.
- [15] G. Buchalla and A. J. Buras, Nucl. Phys. B **548**, 309 (1999), hep-ph/9901288.
- [16] J. Brod, M. Gorbahn, and E. Stamou, Phys. Rev. D **83**, 034030 (2011), 1009.0947.
- [17] X. G. He and G. Valencia, Phys. Lett. B **821**, 136607 (2021), 2108.05033.
- [18] D. M. Straub (2018), 1810.08132.
- [19] A. J. Davies and X.-G. He, Phys. Rev. D **43**, 225 (1991).
- [20] S. Davidson, D. C. Bailey, and B. A. Campbell, Z. Phys. C **61**, 613 (1994), hep-ph/9309310.
- [21] R. Bause, H. Gisbert, M. Golz, and G. Hiller, JHEP **12**, 061 (2021), 2109.01675.
- [22] N. Rajeev and R. Dutta, Phys. Rev. D **105**, 115028 (2022), 2112.11682.
- [23] R. Aaij et al. (LHCb), Phys. Rev. Lett. **131**, 051803 (2023), 2212.09152.
- [24] B. Capdevila, A. Crivellin, and J. Matias (2023), 2309.01311.
- [25] U. Laa, D. Cook, and G. Valencia, Statistics **29**, 681 (2020), 1910.10854.
- [26] U. Laa and G. Valencia, Eur. Phys. J. Plus **137**, 145 (2022), 2103.07937.
- [27] U. Laa, A. Aumann, D. Cook, and G. Valencia, Journal of Computational and Graphical Statistics **32**, 1229 (2023), <https://doi.org/10.1080/10618600.2023.2206459>, URL <https://doi.org/10.1080/10618600.2023.2206459>.
- [28] R. L. Workman et al. (Particle Data Group), PTEP **2022**, 083C01 (2022).
- [29] X.-G. He and G. Valencia, Phys. Rev. D **66**, 013004 (2002), [Erratum: Phys.Rev.D 66, 079901 (2002)], hep-ph/0203036.
- [30] X.-G. He and G. Valencia, Phys. Lett. B **779**, 52 (2018), 1711.09525.
- [31] X.-G. He and G. Valencia, Phys. Rev. D **70**, 053003 (2004), hep-ph/0404229.
- [32] X.-G. He and G. Valencia, Phys. Rev. D **74**, 013011 (2006), hep-ph/0605202.
- [33] G. Li and J. Tandean (2023), 2306.05333.
- [34] Y. Liao, X.-D. Ma, and Q.-Y. Wang, JHEP **08**, 162 (2020), 2005.08013.
- [35] X.-G. He, X.-D. Ma, and G. Valencia, JHEP **03**, 037 (2023), 2209.05223.
- [36] J. F. Kamenik and C. Smith, JHEP **03**, 090 (2012), 1111.6402.
- [37] W. G. Parrott, C. Bouchard, and C. T. H. Davies ((HPQCD collaboration)§, HPQCD), Phys. Rev. D **107**, 014510 (2023), 2207.12468.
- [38] P. Ball and R. Zwicky, Phys. Rev. D **71**, 014015 (2005), hep-ph/0406232.
- [39] A. Bharucha, D. M. Straub, and R. Zwicky, JHEP **08**, 098 (2016), 1503.05534.
- [40] Y. Liao and X.-D. Ma, Phys. Rev. D **96**, 015012 (2017), 1612.04527.
- [41] T. Felkl, S. L. Li, and M. A. Schmidt, JHEP **12**, 118 (2021), 2111.04327.
- [42] G. Li, T. Wang, Y. Jiang, J.-B. Zhang, and G.-L. Wang, Phys. Rev. D **102**, 095019 (2020), 2004.10942.
- [43] N. Gubernari, A. Kokulu, and D. van Dyk, JHEP **01**, 150 (2019), 1811.00983.